Species separation in inertial confinement fusion fuels

C. Bellei, P. A. Amendt, S. C. Wilks, M. G. Haines, D. T. Casey et al.

Citation: Phys. Plasmas **20**, 012701 (2013); doi: 10.1063/1.4773291
View online: http://dx.doi.org/10.1063/1.4773291
View Table of Contents: http://pop.aip.org/resource/1/PHPAEN/v20/i1
Published by the American Institute of Physics.

Species separation in inertial confinement fusion fuels

C. Bellei,[1] P. A. Amendt,[1] S. C. Wilks,[1] M. G. Haines,[2] D. T. Casey,[1,3] C. K. Li,[3] R. Petrasso,[3] and D. R. Welch[4]
[1]*Lawrence Livermore National Laboratory, 7000 East Avenue, Livermore, California 94550, USA*
[2]*The Blackett Laboratory, Imperial College, London SW7 2AZ, United Kingdom*
[3]*Plasma Science and Fusion Center, Massachusetts Institute of Technology, Cambridge, Massachusetts 02139, USA*
[4]*Voss Scientic, Albuquerque, New Mexico 87108, USA*

(Received 16 October 2012; accepted 11 December 2012; published online 3 January 2013)

It is shown by means of multi-fluid particle-in-cell simulations that convergence of the spherical shock wave that propagates through the inner gas of inertial confinement fusion-relevant experiments is accompanied by a separation of deuterium (D) and tritium (T) ions across the shock front. Deuterons run ahead of the tritons due to their lower mass and higher charge-to-mass ratio and can reach the center several tens of picoseconds before the tritons. The rising edge of the DD and TT fusion rate is also temporally separated by the same amount, which should be an observable in experiments and would be a direct proof of the "stratification conjecture" on the shock front [Amendt *et al.*, Phys. Plasmas **18**, 056308 (2011)]. Moreover, dephasing of the D and T shock components in terms of density and temperature leads to a degradation of the DT fusion yield as the converging shock first rebounds from the fuel center (shock yield). For the parameters of this study, the second peak in the fusion yield (compression yield) is strongly dependent on the choice of the flux limiter. © *2013 American Institute of Physics*. [http://dx.doi.org/10.1063/1.4773291]

I. INTRODUCTION

In inertial confinement fusion (ICF), fusion reactions are achieved by compressing a spherical shell composed of deuterium and tritium (DT) to ion temperatures $>10\,\mathrm{keV}$ and areal densities $\rho R > 0.3\,\mathrm{g/cm^2}$. Compression of the initially cold shell is achieved by launching a series of intense shock waves that are either driven by a laser beam (direct-drive ICF) or by a bath of soft x rays (indirect-drive ICF). These shock waves should coalesce near the inner surface of the DT ice layer to minimize entropy production in the fuel.[1] After shock coalescence, the resulting, converging strong shock passes through the rapidly ionized inner fuel gas and effectively propagates through a fully ionized DT plasma composed of distinct species: electrons, deuterons, and tritons.

To date, most of the work that is carried out in the ICF community is with average-atom radiation-hydrodynamic (RH) codes. In practice, these codes solve one equation of continuity, one momentum equation and (typically) two energy equations for electrons and the average-DT ion species, using an equation-of-state. This approach assumes that there is exact charge neutrality ($n_e = n_{DT}$) and neglects several effects which are potentially important in various stages of an ICF implosion: the presence of electric (and magnetic) fields, binary diffusion of ion species, and kinetic effects.

Indeed, there is increasing experimental evidence for the necessity of including physics models beyond the average-atom fluid approach: electric fields of 1–10 GV/m have been inferred during the implosion of ICF capsules on the OMEGA facility at the Laboratatory for Laser Energetics[2,3] and anomalies in the fusion yield have been conjectured as a consequence of species separation,[4] in the absence of other compelling explanations. More recently, the effect of the ion mean free paths when the hot spot is formed has been considered.[5]

Seminal work by Jukes,[6] Shafranov,[7] and Jaffrin and Probstein[8] has shown that the structure of a shock wave in a plasma can significantly differ from the structure of a gas-dynamical shock, essentially due to the different scale-lengths of the problem: While in the latter case the width of the shock is determined by the molecular mean-free-path, in the former case there are at least two scale lengths: the electron-ion mean free path for thermal equilibration (Δ_{ei}) and the ion-ion mean free path for large angle scattering (λ_{ii}). Due to the lower electron mass, the heat flow is dominated by the electron thermal conduction, although ions may carry a non-negligible fraction of it,[9] while viscous effects are dominated by the ion species at high Mach number.

Figure 1 shows the magnitude of these scale lengths for the case of a spherical shock that converges in a DT gas. This plot is obtained using a self-similar Guderley solution[10,11] of a converging spherical shock under conditions relevant to ignition experiments on the National Ignition Facility (NIF). The quantity Δ_{ei} determines the scale length of the heat conduction front ahead of the shock and of the thermalization layer behind the shock; it is substantially larger than λ_{ii} (by about a factor $\sqrt{m_i/m_e}$) which determines the scale length of the ion viscous forces. When the shock reaches $r \sim 100\,\mu\mathrm{m}$, the conduction front has already reached the origin; when $r \sim 30\,\mu\mathrm{m}$, the leading edge of the viscous layer reaches the origin. These effects can, in principle, be represented in standard ICF codes, by setting the right amount of flux limiter (for the thermalization part) and artificial viscosity (for the viscous part), provided also that the grid resolution is smaller than λ_{ii}.

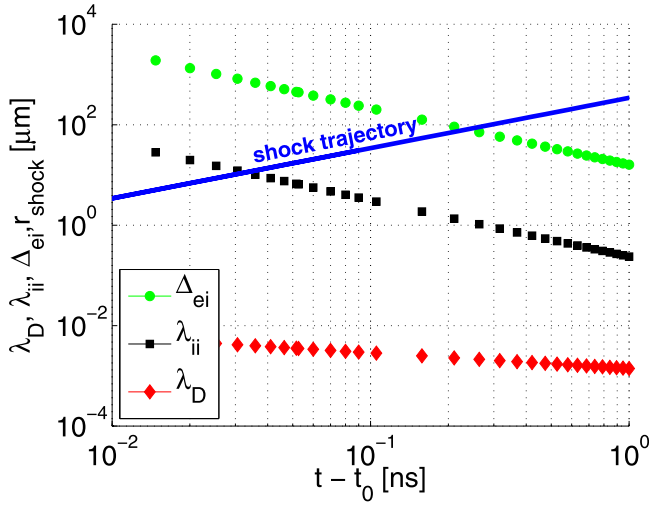

FIG. 1. Debye (λ_D) and collisional ($\Delta_{ei}, \lambda_{ii}$) scale lengths during convergence of a shock in spherical geometry, for ignition-relevant parameters, relative to the time of shock flash t_0. Numerical values are obtained from a Guderley solution for a Mach M = 10 shock at r = 1 mm that propagates through a DT gas with initial temperature $T = 5$ eV and mass density $\rho = 0.01$ g/cc.

The next level of complication is the inclusion of multiple ion species, which introduces new scale lengths. Experimental[12] and theoretical[13,14] work has investigated the structure of shock waves in neutral gas mixtures; however, to our knowledge no studies have been made for the case of gas mixtures in plasmas, particularly in the field of ICF.

Multi-species calculations of ICF implosions have been recently presented at international conferences:[15,16] this paper is, essentially, a summary of that work. More specifically, in this paper separation of D and T ions is shown to occur during shock convergence in the inner gas of an ICF capsule, according to multi-fluid particle-in-cell simulations, lowering the DT yield around shock flash.

The structure of this paper is as follows. In the first part, the possibility of having a non-zero ion drift speed in a quasi-neutral plasma is motivated by simple analytical arguments. Numerical examples of shock wave propagation in a ternary gas mixture (two ions, one electron species) will be shown to potentially lead to the formation of distinct ion shock features. These effects are also present in more realistic simulations of OMEGA exploding pusher experiments, with clear signatures in the predicted fusion burn history. In "exploding pusher" implosions, the spherical target is typically made of a CH or glass shell that is only a few microns thick; the target is then filled with different gases such as DT or D^3He. Heating of the shell by the radiation field generates a strong shock that propagates through the inner gas, converging towards the center and providing a relatively large "shock-flash yield" compared to the "compression yield," as it will be discussed in Sec. IV. Exploding pusher experiments are of interest for shock physics studies.

II. DIFFUSION IN A BINARY MIXTURE AND IN A MULTI-COMPONENT PLASMA

In a binary mixture of gases, diffusion of the two components is described by the equation[17]

$$\mathbf{u}_1 - \mathbf{u}_2 = -\frac{D}{x(1-x)}\left\{\nabla x + \frac{n_1 n_2 (m_2 - m_1)}{n\rho}\nabla \ln p - \frac{\rho_1 \rho_2}{p\rho}(\mathbf{F}_1 - \mathbf{F}_2) + k_T \nabla \ln T\right\}. \quad (1)$$

In this equation, $\mathbf{u}_1$ and $\mathbf{u}_2$ are the fluid velocities of the two components; D is a diffusion coefficient; $x = n_1/(n_1 + n_2)$ is the molecular fraction of species 1; $n = n_1 + n_2$, $\rho = \rho_1 + \rho_2$, and $p = p_1 + p_2$ are the total number density, mass density, and pressure of the mixture, respectively; m_1 and m_2 are the respective masses; $\mathbf{F}_1$ and $\mathbf{F}_2$ are the forces per unit mass exerted upon the molecules of the two components; k_T is a thermal diffusion factor and T is the temperature, assumed the same for the two species. A similar result is obtained for the case of a ternary mixture in a plasma,[18] with the qualitative picture remaining the same: In the presence of gradients in the thermodynamic variables, such as across a shock front, species diffusion can occur.

Under the quasi-neutral approximation, it is easy to show that in a *binary* plasma (electrons and ions) the electron-ion drift speed can be neglected at once, compared to the average fluid velocity. For this purpose, it suffices to write the continuity equations for the electron and ion species

$$\frac{\partial n_e}{\partial t} + \nabla \cdot (n_e \mathbf{u}_e) = 0,$$

$$\frac{\partial n_i}{\partial t} + \nabla \cdot (n_i \mathbf{u}_i) = 0.$$

After using the quasi-neutral approximation, $Z_i n_i = n_e$, subtraction of the two equations above leads to the condition $\nabla \cdot \mathbf{j} = 0$ for the local current density $\mathbf{j}$. In 1D geometry, the only meaningful solution is $j = 0$ which leads to $u_e = u_i$, i.e., electrons and ions cannot appreciably separate.

To justify the quasi-neutral approximation, note that $(Z_i n_i - e n_e)/e n_e$ is on the order of the square of the ratio between the Debye length and the ion mean free path, $(\lambda_D/\lambda_{ii})^2$. This quantity is typically $\ll 1$ in ICF plasmas (see Figure 1), although it is worth pointing out that there is an important exception during NIF implosions: As the main fuel is compressed by the four shocks launched at the outer surface of the shell's ablator, its mass density is of about 1 g/cc and its temperature is between 5 and 10 eV. In this (warm dense matter) regime, the quantity $(\lambda_D/\lambda_{ii})^2$ is of order unity and a non-negligible current may occur in this circumstance.

In a multi-component plasma, the situation can be drastically different than in a single-ion plasma. Indeed, in this case there are essentially more degrees of freedom that can guarantee the quasi-neutrality condition to be fulfilled without stringent requirements on the drift speeds. After writing the continuity equation for n different species in 1D, the constraint on the fluid velocities becomes

$$Z_1 n_1 (u_1 - u_e) + \cdots + Z_n n_n (u_n - u_e) = 0.$$

The implication of the equation above is precisely that the current density is negligible in this case too, since under the quasi-neutral approximation $j = Z_1 n_1 (u_1 - u_e) + \cdots$

$+Z_n n_n(u_n - u_e)$. However, provided that $j=0$, in this case a drift speed between the different components is now allowed.

To understand how different components of a plasma can react differently and lead to separation of the species, consider the following classic example in gas dynamics: the generation of a shock wave by the instantaneous acceleration of a piston to a constant velocity v_p. In the limit of instant acceleration, the compression waves that are produced by the movement of the piston coalesce all at $t=0$, and a shock wave is instantly produced that travels at a velocity $v_s > v_p$. After using the Rankine-Hugoniot relations for the upstream and downstream flow speeds and imposing that the downstream velocity equals the piston velocity, the shock speed can be found analytically to be

$$v_s = \frac{\gamma+1}{4} v_p + \left[\left(\frac{\gamma+1}{4} v_p \right)^2 + a_0^2 \right]^{1/2}, \qquad (2)$$

where $\gamma = c_p/c_v$ is the ratio of heat capacities and a_0 is the initial speed of sound of the gas. The interest in this formula is that the speed of sound a_0 depends on the molecular weight $\mathcal{M}$ of the gas, through $a_0 = \sqrt{\gamma k_B T/\mathcal{M}}$.

Suppose now that the piston is accelerated in a mixture of n different gases at the same temperature. In a thought experiment, the interaction between the different gases can be considered negligible. In this case, Eq. (2) dictates that the solution of the problem is that n shocks are generated, with distinct velocities $v_{s1}, \ldots, v_{sn}$. The fastest shock is for the gas with the lighter molecular weight. Moreover, the strength of the shock is also different for the different components since the Mach number of the shock, $M = v_s/a_0$, will also be dependent on the molecular weight and, in fact, will be larger the heavier the gas.

The example just given is a simple demonstration that the generation of separate shocks can, at least in principle, occur. Inter-species collisions do complicate the problem significantly, but as it will be shown in Sec. III and IV, under the right conditions the presence of distinct shocks is validated by simulations.

The shock separation depends on the collisionality of the system and on the speed of the shock. Indeed, suppose that a shock of one ion species (species 2) is propagating through a stationary plasma composed of two ion species and neutralizing electrons. In the shock frame, upstream ions of both species enter the shock at the speed v_s. Ions of species 1 are slowed down to the downstream velocity of ions 2 within the distance $\Delta_{\max} \sim v_s/\nu_{12}$, where ν_{12} is the slowing down collision frequency between the two species. The quantity $\Delta_{\max}$ is the mean-free-path of the un-shocked ions of type 1 in the shocked ions of type 2; it can be regarded as the maximum distance over which two shocks may exist.

It is interesting to evaluate the quantity $\Delta_{\max}$ for the same self-similar Guderley solution shown in Figure 1. Figure 2 shows that as the shock propagates to the fuel center the separation can become substantial. For the nominal DT mass density of the inner gas, $\rho = 0.01\,\mathrm{gcm}^{-3}$, the D and T shocks can separate by several tens of microns for $r <$ 200 μm (blue curve). Lowering the density decreases the collision frequency, allowing for larger values of $\Delta_{\max}$ (red curve). Similarly, higher charge states increase the inter-species friction. As a result, *ceteris paribus* (i.e., for otherwise identical conditions) a D^3He plasma should show reduced separation (green curve).

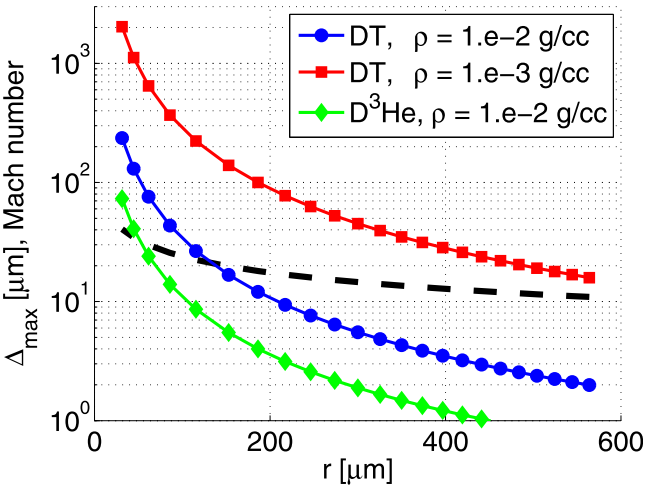

FIG. 2. Maximum separation $\Delta_{\max}$ between two shocks of distinct ion species, for the same Guderley solution shown in Fig. 1. The figure also shows the value of the Mach number as the shock converges towards the center (broken line).

Section III will show how significant drift speeds can occur in both slab and spherical geometries, according to simulation results.

III. SPECIES SEPARATION IN RIEMANN PROBLEMS

It is a classic problem in gas dynamics to find the solution after a diaphragm that separates one gas under two distinct thermodynamic conditions is instantly removed. In general a shock wave, a contact discontinuity and a rarefaction wave are produced. This problem is used in the present manuscript to produce a shock wave in a simulation environment.

The code used throughout this paper is the hybrid-PIC code Lsp.[19,20] For the purpose of this work, the collision operator in Lsp was tested in three different ways: via a Sod test tube problem[21] (in fact, a particular kind of Riemann problem), a thermalization problem, and a slowing down problem. The fusion package was also tested for the case of Maxwellian distribution functions.

In these examples, to separate out effects of thermal conduction the flux limiter for the electron species was kept to a very small value, $f = 10^{-8}$. Significant heat flux can otherwise change the structure of a Riemann problem.

Simulations were run in both slab and spherical geometry, with the purpose of investigating the effects of mass difference, charge state, and background density on the separation of species. Figure 3 presents a comparison between a Hydra[22] solution and a Lsp solution of a Riemann problem, with an initial jump in density of 4× and an initial jump in temperature of 10×. The Lsp calculation, which was initialized with one electron and one ion fluid species, shows good agreement with the Hydra solution.

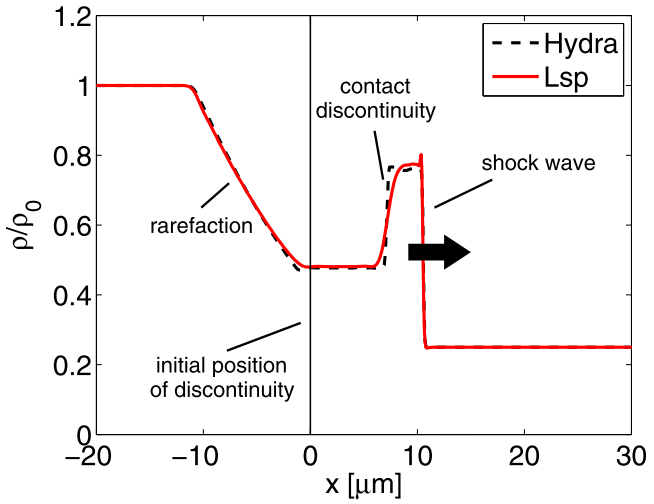

FIG. 3. Comparison of Hydra solution vs. (fluid) Lsp solution of the Riemann problem discussed in the text. When Lsp is run in fluid mode, the solution is close to the expected gas dynamics solution.

Multi-fluid calculations reveal a much richer structure than in single ion species fluid calculations. Figure 4 compares results from the same Riemann problem, but with different compositions of the gas mixture. The simulations were initialized with the following choice of parameters:

$$\begin{cases} x < 0\,\mu\text{m} : \sum_i n_i = 4.0\times10^{19}\,\text{cm}^{-3}; T = 100\,\text{eV} \\ x > 0\,\mu\text{m} : \sum_i n_i = 1.0\times10^{19}\,\text{cm}^{-3}; T = 10\,\text{eV} \end{cases}, \quad (3)$$

where the summation Σ_i is over the ion species, the initial temperature T is the same for all species and, for the two ion species, the ion densities are equal at $t=0$. The initial electron density follows directly from the condition of local charge neutrality, $n_e = \sum_i Z_i n_i$. In Fig. 4(a), the result for a single ion species of mass $\mu = m_i/m_p = 6$ and $Z=1$ is presented. Figures 4(b)–4(d) were initialized with two ion species; cases 4(b) and 4(c), in particular, should be directly compared to case 4(a), since the average mass is the same. Case 4(d) is relevant to a DT plasma; it shows the least separation because of the small difference in the atomic weight of the ions. As Fig. 4 demonstrates, there is a clear dependence of the separation on the mass difference and charge state. This can be related to the barodiffusion and electrodiffusion mechanisms.[18,23]

Figure 4 also shows the estimated value of $\Delta_{\max} = v_s/\nu_{12}$ at the time $t=150$ ps, calculated with standard transport theory and for the different parameters of the simulations. The trend in $\Delta_{\max}$ is consistent with the simulation results and this conclusion still stands in preliminary simulations with fully kinetic ions.

Simulations in spherical geometry were also performed. Spherical geometry makes the problem intrinsically time-dependent. For the same initial conditions, species separation should be more easily observed in this geometry, as the strength of the shock rapidly increases with convergence.

Here, the dependence of the separation on the background density was investigated. In particular, the following Riemann problem for a DT plasma was initialized:

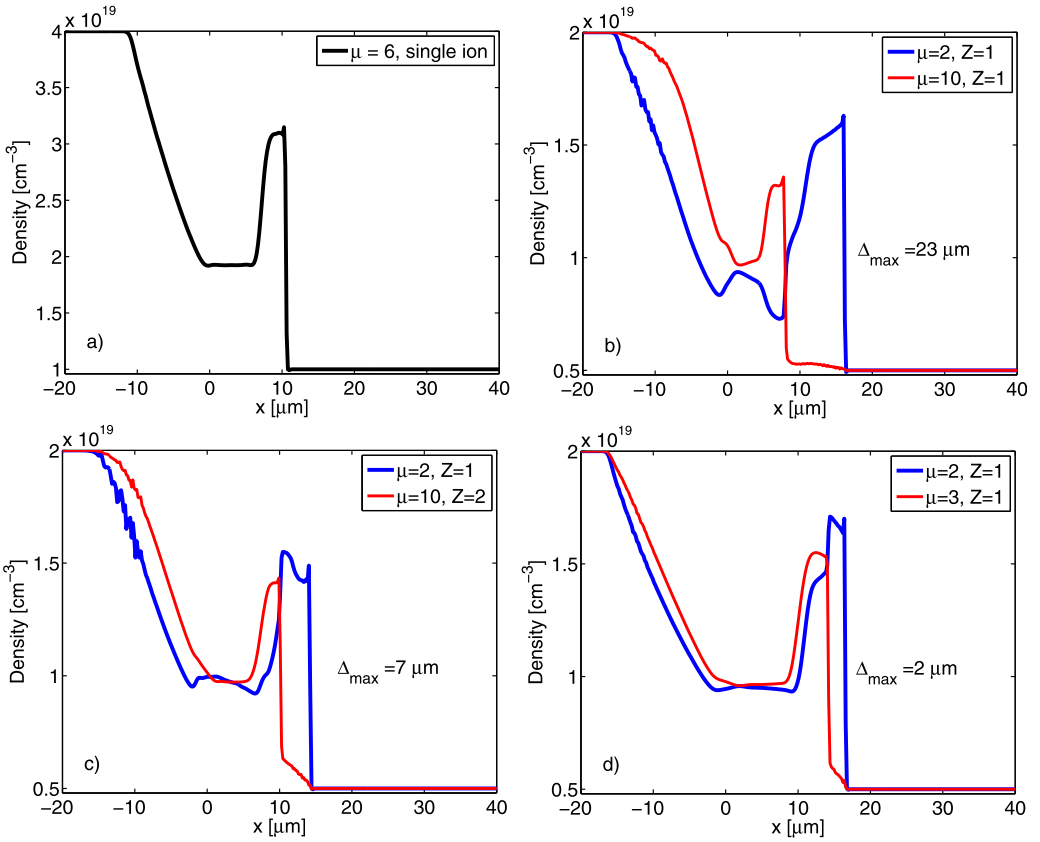

FIG. 4. Particle number density plots from the same Riemann problem in slab geometry, but with different initializations of masses and charge states (see legend). The Mach number of the shock produced in this problem is $M \simeq 2$. All the panels refer to the same time $t=150$ ps. The quantity μ represents the ratio of the ion mass over the proton mass. In simulation (a), a single ion species was used with mass $\mu=6$. Simulations (b), (c) and (d) were initialized with two ion species.

$$\begin{cases} r < 40\,\mu\text{m} : n_d = n_t = 5.0 \times 10^{20}\text{cm}^{-3}(a), 1.25 \times 10^{20}\,\text{cm}^{-3}(b); T = 10\,\text{eV} \\ r > 40\,\mu\text{m} : n_d = n_t = 3.0 \times 10^{21}\text{cm}^{-3}(a), 7.50 \times 10^{20}\,\text{cm}^{-3}(b); T = 100\,\text{eV} \end{cases}, \quad (4)$$

where, as before, the electron particle number density can be found from the charge neutrality condition, $n_e = n_D + n_T$, and the temperature T is the same for all species.

As shown in Figure 5, the separation of D and T ions is more evident in the low density case: Separation of species can occur in a DT plasma, if the Mach number of the shock is high enough and the densities are low enough.

IV. ICF-RELEVANT SIMULATIONS

Based on the estimates from Fig. 2 and on the numerical experiments shown in Sec. III, the following conclusion can be drawn: Species separation should be evident during shock convergence in the inner DT gas of an imploding shell. In fact, while the densities are of the same order of magnitude as in the examples of Fig. 5, shock speeds are substantially higher (in the range of several hundreds km/s, with Mach number up to $M \simeq 50$ just before shock flash), so the effect should be enhanced.

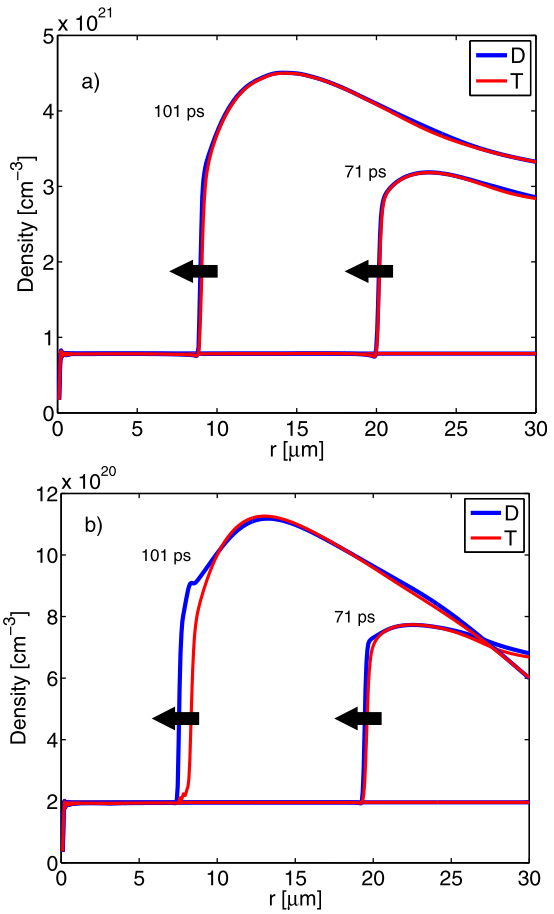

FIG. 5. Results from a Riemann problem in spherical geometry, with parameters given by Eq. (4). Case (a) and (b) differ in that case (b) was initialized with a reduction of density by 4 × with respect to case (a). The Mach number of the shock at $t = 71$ ps and $t = 101$ ps is $M = 2.6$ and $M = 2.8$, respectively.

With this is mind, it is clear that exploding pusher experiments are an ideal platform to test the physics beyond the single ion species approximation. Indeed, for these experiments the shock yield can be unambiguously determined due to minimal compression yield. The interpretation of the results is also aided by the fact that there are virtually no issues with mix and implosion symmetry that plague the compressional burn phase. Thus, fusion yield anomalies due to species separation are expected to be a clear signature of these experiments.

To prove this point, a Lsp simulation was set up from a Lilac[24] calculation of shot 58163 on OMEGA. The capsule, with a diameter of 1600 μm, was made of a SiO_2 shell of thickness 3.8 μm and filled with a DT mixture at 10.1 atm, with an initialized atomic fraction of tritium atoms over deuterium atoms $f_T/f_D = 0.62$. Implosion of the capsule was achieved by shining 60 laser beams on target, with a total energy of 28 kJ delivered in a 1 ns square pulse.

The Lilac profiles at time $t = 1$ ns, i.e., at the end of the laser pulse (Fig. 6), were used to initialize a Lsp multi-fluid calculation. To decrease the run time of the simulation, all the species were treated as fluid particles, i.e., assuming Maxwellian velocity distributions. This comes at the cost of

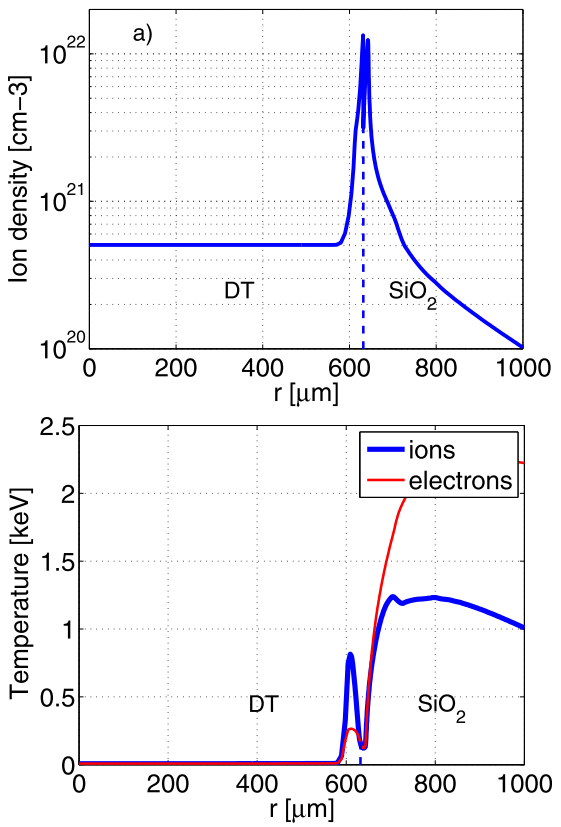

FIG. 6. Lilac profiles at the end of the OMEGA laser pulse (1 ns), for shot 58163. These profiles were used to initialize a Lsp calculation. Data courtesy of P. B. Radha, LLE.

decreased accuracy in the evaluation of inter-species collisional effects. Future work will address in detail the effects of kinetics during ICF implosions. This will require a substantially larger number of simulation particles, in order to accurately represent an arbitrary velocity distribution.

Particle density plots (Fig. 7) show that, as time progresses, the separation increases substantially. At $t = 1650$ ps, the deuteron shock reaches the origin; the tritium shock lags behind by more than $100\,\mu$m and reaches the center at $t = 1730$ ps. It is also interesting to note how the presence of an electric field can substantially modify the structure of the shock, because the electric field of the slower shock can compress the light ions ahead. The result is that an abrupt decrease in the D density appears at the location of the T shock, as pointed out in the figure. This mechanism of compression of the lighter ions induced by the electric field can also be appreciated in Fig. 4.

The separation of D and T ions is also confirmed by the temperature and electric field plots (Fig. 8). In the temperature plots, note that at late times the peak temperature of the deuterium is substantially higher than the tritium one. This is simply due to the fact that, at a given time, the deuterium has converged further towards the center. At earlier times (see snapshot at 1190 ps), when the separation is still negligible and the shock speeds are nearly the same, the heavier species (tritium) exhibits a higher peak temperature; this is expected from a simple argument of energy conservation, as the upstream flux of kinetic energy $F_k = \rho v^2/2$ is proportional to the species mass. Note also the thermalization occurring between D and T ions, most evident in the snapshot at 1640 ps behind the D shock and ahead of the T shock.

As the shock strengthens during convergence, the peak electric field of the D shock increases to above 1 GV/m; this magnitude is consistent with what inferred from experiments.[2,3] The presence of multiple peaks in the electric field structure is also a signature of the presence of multiple shocks.

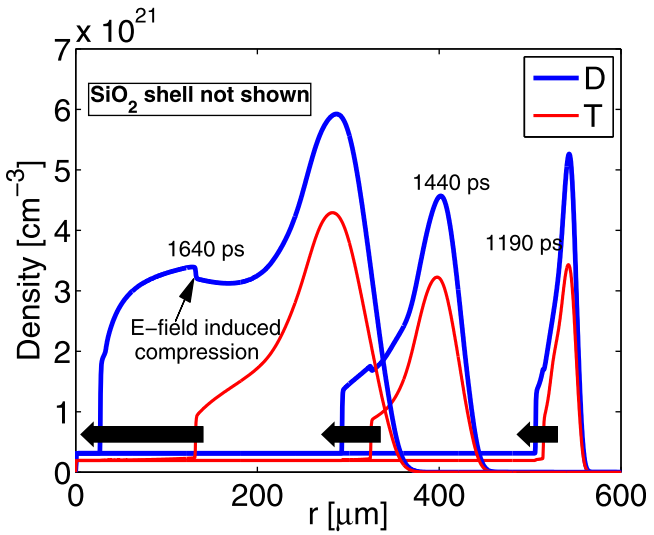

FIG. 7. Particle density of deuterons and tritons at three different snapshots from the beginning of the implosion (the electron flux limiter for this simulation was $f = 0.2$). Note that the unperturbed number density is different for the two species, since $f_T/f_D = 0.62$ for this shot.

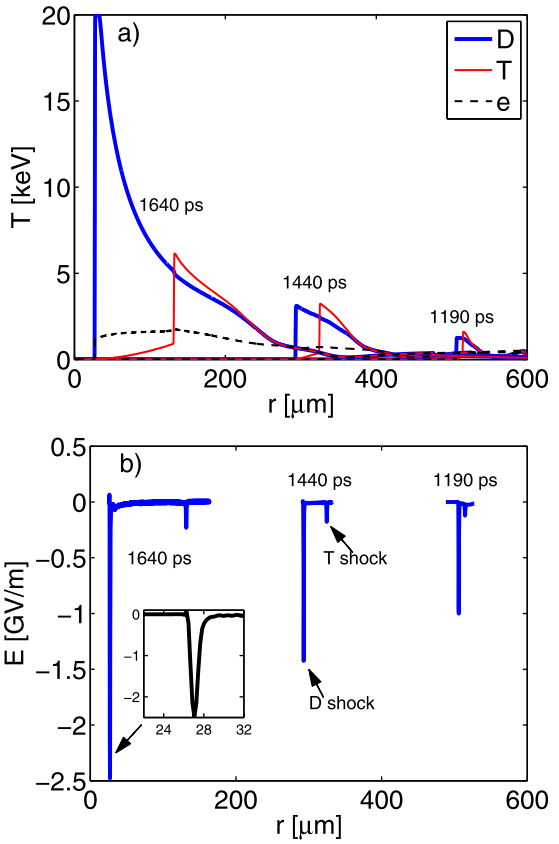

FIG. 8. Temperature (a) and electric field (b) profiles at different times (electron flux limiter $f = 0.2$). The inset in panel (b) is a magnified plot of the electric field across the D shock, at $t = 1640$ ps. In the convention used here, a negative electric field points towards the origin, $r = 0$.

Separation of deuterons and tritons has as immediate effect at "shock flash" in the fusion burn history, i.e, after the converging shock first rebounds from the center. It is easy to see this after recalling the dependences of the DT reaction rate $Y_{DT} \sim n_D n_T \langle \sigma v \rangle$. When species separation occurs, both the peak in density and the peak in temperature are out of phase. This reduces the product $n_D n_T$ at any given time; also, the reactivity $\langle \sigma v \rangle$ is reduced since the maximum reactivity occurs for D and T ions of similar temperature. As a consequence, a lowering in the DT shock yield is expected, which is what is found in the simulations of Fig. 9 (for shock yield, it is meant the first peak in the fusion burn history). Note that in the simulations shown here the reactivity calculations did not assume the D and T ions to have the same temperature, as it is implicitly assumed in mainline ICF codes.

The other signature of species separation is that at shock flash the rising edge and peak of the DD and TT fusion yields are well separated in time, independently of the choice of the flux limiter. In the right column of Figure 9, the rising edges are separated by about 100 ps, which could be measurable in experiments and would be a direct confirmation of the "stratification conjecture" on the shock front.[25]

The flux limiter has an effect on the second peak of the fusion yield, the so-called "compression yield," which is produced when the rebound shock is reflected back from the

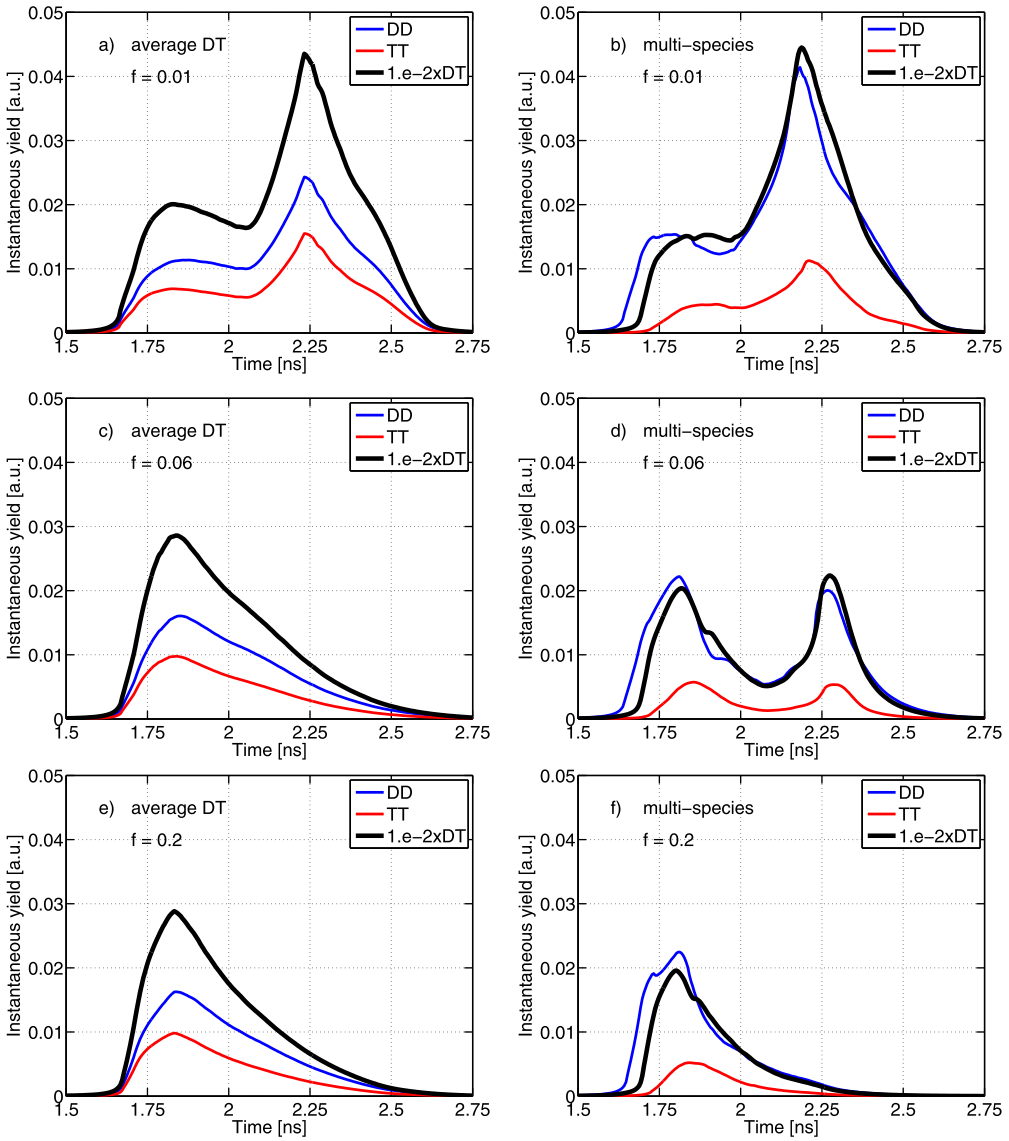

FIG. 9. Fusion rates for the exploding pusher simulation described in the text (times are relative to the beginning of the implosion), for the two cases of an average-ion calculation (left column) and a two-species calculation (right column) and for different values of the electron flux limiter $f = 0.01$, 0.06, 0.2. The left peak in the fusion yield is what is referred to as "shock yield" in the text, as opposed to the "compression yield" peak on the right.

outer shell. This peak is seen to reduce strongly with increasing value of the flux limiter f. The reason is that a larger value of f implies a higher heat flux between the hot center and the surrounding, colder plasma; this can quench fusion reactions at late times. It is also interesting to note how the multi-fluid and average-species descriptions can respond differently to the value of the flux limiter (Figs. 9(c) and 9(d)), particularly in the region of $f = 0.06$ which represents a typical value used in radiation hydrodynamics codes.

V. CONCLUSIONS

Multi-species simulations of ICF-relevant experiments show separation of D and T ions during convergence of the shock in the inner DT gas of an ICF capsule. Distinct ion shocks can be observed in the simulations, depending on the ion-ion coupling and on the strength of the shock. Lower densities and higher Mach numbers increase the separation.

In exploding pusher implosions, the predicted main effect of species separation is a decrease in the DT fusion yield at shock flash (shock yield); at the same time, the DD yield is seen to increase, while the TT yield is reduced. The time differential between DD and TT shock yields could be measured experimentally to give conclusive experimental evidence for species separation. The DT, DD, and TT "compression yields" can also be affected by multi-species physics, but here there is also a strong dependence on the choice of the flux limiter.

For this reason and since the actual separation between ion species is closely dependent on the correct modeling of the collision physics, fully kinetic (particle-in-cell) simulations of ICF experiments are needed to further investigate the effects of multi-species.

In conclusion, this work suggests the need for adapting mainline ICF simulations to include ion separation and kinetic effects in mixed species fuels. The implications of

species separation for current ignition experiments on the National Ignition Facility are under investigation.

ACKNOWLEDGMENTS

Useful discussions with D. Ryutov and E. Williams are acknowledged. The authors also thank P. B. Radha for providing Lilac simulation results. Computing support for this work came from a LLNL Computational Directorate Grand Challenge award.

This work was performed under the auspices of the U.S. Department of Energy by the Lawrence Livermore National Laboratory under Contract No. DE-AC52-07NA27344 and supported by LDRD-11-ERD-075.

[1]J. D. Lindl, P. Amendt, R. L. Berger, S. Gail Glendinning, S. H. Glenzer, S. W. Haan, R. L. Kauffman, O. L. Landen, and L. J. Suter, "The physics basis for ignition using indirect-drive targets on the National Ignition Facility," Phys. Plasmas **11**(2), 339–491 (2004).

[2]J. R. Rygg, F. H. Séguin, C. K. Li, J. A. Frenje, M. J.-E. Manuel, R. D. Petrasso, R. Betti, J. A. Delettrez, O. V. Gotchev, J. P. Knauer, D. D. Meyerhofer, F. J. Marshall, C. Stoeckl, and W. Theobald, "Proton radiography of inertial fusion implosions," Science **319**(5867), 1223–1225 (2008).

[3]C. K. Li, F. H. Séguin, J. R. Rygg, J. A. Frenje, M. Manuel, R. D. Petrasso, R. Betti, J. Delettrez, J. P. Knauer, F. Marshall, D. D. Meyerhofer, D. Shvarts, V. A. Smalyuk, C. Stoeckl, O. L. Landen, R. P. J. Town, C. A. Back, and J. D. Kilkenny, "Monoenergetic-proton-radiography measurements of implosion dynamics in direct-drive inertial-confinement fusion," Phys. Rev. Lett. **100**, 225001 (2008).

[4]D. T. Casey, J. A. Frenje, M. Gatu Johnson, M. J.-E. Manuel, H. G. Rinderknecht, N. Sinenian, F. H. Séguin, C. K. Li, R. D. Petrasso, P. B. Radha, J. A. Delettrez, V. Yu Glebov, D. D. Meyerhofer, T. C. Sangster, D. P. McNabb, P. A. Amendt, R. N. Boyd, J. R. Rygg, H. W. Herrmann, Y. H. Kim, and A. D. Bacher, "Evidence for stratification of deuterium-tritium fuel in inertial confinement fusion implosions," Phys. Rev. Lett. **108**, 075002 (2012).

[5]K. Molvig, N. M. Hoffman, B. J. Albright, E. M. Nelson, and R. B. Webster, "Knudsen layer reduction of fusion reactivity," Phys. Rev. Lett. **109**, 095001 (2012).

[6]J. D. Jukes, "The structure of a shock wave in a fully ionized gas," J. Fluid Mech. **3**(03), 275–285 (1957).

[7]V. D. Shafranov, "The structure of shock waves in a plasma," Sov. Phys. JETP **5**, 1183 (1957).

[8]M. Y. Jaffrin and R. F. Probstein, "Structure of a plasma shock wave," Phys. Fluids **7**(10), 1658–1674 (1964).

[9]M. Casanova, O. Larroche, and J. -Pierre Matte, "Kinetic simulation of a collisional shock wave in a plasma," Phys. Rev. Lett. **67**, 2143–2146 (1991).

[10]Ya. B. Zel'dovich and Yu. P. Raizer, *Physics of Shock Waves and High-Temperature Phenomena* (Dover, Mineola, NY, 2002).

[11]S. Atzeni and J. Meyer-Ter-Vehn, *The Physics of Inertial Fusion* (Oxford University Press, 2004).

[12]R. E. Center, "Measurement of shock-wave structure in helium-argon mixtures," Phys. Fluids **10**(8), 1777–1784 (1967).

[13]F. S. Sherman, "Shock-wave structure in binary mixtures of chemically inert perfect gases," J. Fluid Mech. **8**(03), 465–480 (1960).

[14]E. Goldman and L. Sirovich, "The structure of shock-waves in gas mixtures," J. Fluid Mech. **35**(03), 575–597 (1969).

[15]C. Bellei, P. A. Amendt, and S. C. Wilks, "Plasma effects in spherical implosions," in APS DPP Conference, 2012.

[16]C. Bellei, P. A. Amendt, S. C. Wilks, M. G. Haines, D. T. Casey, C. K. Li, and R. Petrasso, "Dependence of the fusion yield on the separation of D and T ions in exploding pusher simulations," in Anomalous Absorption Conference, 2011.

[17]S. Chapman and T.G. Cowling, *The Mathematical Theory of Non-Uniform Gases*, 3rd ed. (Cambridge University Press, 1970).

[18]G. Kagan and X. -Zhu Tang, "Electro-diffusion in a plasma with two ion species," Phys. Plasmas **19**(8), 082709 (2012).

[19]T. P. Hughes, R. E. Clark, and S. S. Yu, "Three-dimensional calculations for a 4 kA, 3.5 MV, 2 microsecond injector with asymmetric power feed," Phys. Rev. ST Accel. Beams **2**, 110401 (1999).

[20]D. R. Welch, D. V. Rose, B. V. Oliver, and R. E. Clark, "Simulation techniques for heavy ion fusion chamber transport," Nucl. Instrum. Methods Phys. Res. A **464**(1–3), 134–139 (2001).

[21]C. B. Laney, *Computational Gasdynamics* (Cambridge University Press, 1998).

[22]M. M. Marinak, G. D. Kerbel, N. A. Gentile, O. Jones, D. Munro, S. Pollaine, T. R. Dittrich, and S. W. Haan, "Three-dimensional hydra simulations of National Ignition Facility targets," Phys. Plasmas **8**(5), 2275–2280 (2001).

[23]P. Amendt, C. Bellei, and S. Wilks, "Plasma adiabatic lapse rate," Phys. Rev. Lett. **109**, 075002 (2012).

[24]J. Delettrez, R. Epstein, M. C. Richardson, P. A. Jaanimagi, and B. L. Henke, "Effect of laser illumination nonuniformity on the analysis of time-resolved x-ray measurements in UV spherical transport experiments," Phys. Rev. A **36**, 3926–3934 (1987).

[25]P. Amendt, S. C. Wilks, C. Bellei, C. K. Li, and R. D. Petrasso, "The potential role of electric fields and plasma barodiffusion on the inertial confinement fusion database," Phys. Plasmas **18**(5), 056308 (2011).